Toxicology and Applied Pharmacology 354 (2018) 215–224

Contents lists available at ScienceDirect

Toxicology and Applied Pharmacology

journal homepage: www.elsevier.com/locate/taap

# Using primary organotypic mouse midbrain cultures to examine developmental neurotoxicity of silver nanoparticles across two genetic strains

Brittany A. Weldon[a,b,1], Julie Juyoung Park[a,b,1], Sungwoo Hong[a,b], Tomomi Workman[a,b], Russell Dills[b], Ji Hyun Lee[b], William C. Griffith[a,b], Terrance J. Kavanagh[b], Elaine M. Faustman[a,b,*]

[a] Institute for Risk Analysis and Risk Communication, University of Washington, Seattle, WA, USA
[b] Department of Environmental and Occupational Health Sciences, University of Washington, Seattle, WA, USA

ARTICLE INFO

*Keywords:*
Silver nanoparticles
Micromass
Developmental neurotoxicity
Dosimetry
*In vitro* nanotoxicology
Genes x environment

ABSTRACT

Micromass culture systems have been developed as three-dimensional organotypic *in vitro* alternatives to test developmental toxicity. We have optimized a murine-based embryonic midbrain micromass system in two genetic strains to evaluate neurodevelopmental effects of gold-cored silver nanoparticles (AgNPs) of differing sizes and coatings—20 nm AgCitrate, 110 nm AgCitrate, and 110 nm AgPVP. AgNPs are increasingly used in consumer, commercial, and medical products for their antimicrobial properties and observations of Ag in adult and fetal brain following *in vivo* exposures to AgNPs have led to concerns about the potential for AgNPs to elicit adverse effects on neurodevelopment and neurological function. Cytotoxicity was assessed at three time points of development by both nominal dose and by dosimetric dose. Ag dosimetry was assessed in cultures and the gold core component of the AgNPs was used as a tracer for determination of uptake of intact AgNPs and silver dissolution from particles in the culture system. Results by both nominal and dosimetric dose show cell death increased significantly in a dose-dependent manner at later time points (days 15 and 22 *in vitro*) that coincide with differentiation stages of development in both strains. When assessed by dosimetric dose, cultures were more sensitive to smaller particles, despite less uptake of Ag in smaller particles in both strains.

## 1. Introduction

Proper function of the central nervous system (CNS) is essential for the survival of humans and many other species. The CNS can be damaged by many environmental and pharmacological toxicants and has been identified as a sensitive target of toxicity in a variety of exposures. The developing nervous system has been shown to be even more susceptible to perturbations than a mature nervous system (Rice and Barone Jr., 2000). Disruption of the development of the CNS can result in lifelong neurological disorders including autism, attention deficit disorder, cerebral palsy, and mental retardation (Grandjean and Landrigan, 2006). The United States National Research Council estimated that one in every six children have the developmental disability, and of these developmental disabilities in children, 25% occur from interactions between environmental factors and individual genetic susceptibility (National Research Council Committee on Developmental Toxicology, 2000). These disorders can put immense strain on individuals, families, the healthcare system, and society. With such broad reaching and powerful implications, it is critical to address the potential for new and novel developments in drugs, chemicals, and other technologies to act as developmental neurotoxicants. Despite this, < 0.01% of chemicals registered with U. S. Environmental Protection Agency (EPA) have been tested for potential developmental neurotoxicity (Miodovnik, 2011), suggesting that there is a pressing need for improved efficiency in toxicity assessment.

Recent technological developments have employed the use of a wide array of nano-scale materials (< 100 nm), referred to generally as Engineered Nanomaterials (ENMs), for their attractive qualities including small size, large surface area, charge, and lightness of weight. These unique properties of ENMs also create the potential for ENMs to interact with biological systems. The utilization of ENMs in medicine, manufacturing, and industry continues to accelerate; however, much is still unknown about their potential for toxicity in many organ systems, including the developing CNS.

* Corresponding author at: Institute for Risk Analysis and Risk Communication, Department of Environmental and Occupational Health Sciences, University of Washington, Seattle, WA, USA.
*E-mail address:* faustman@u.washington.edu (E.M. Faustman).
[1] These authors contributed equally to the manuscript.

https://doi.org/10.1016/j.taap.2018.04.017
Received 2 November 2017; Received in revised form 10 April 2018; Accepted 13 April 2018
Available online 17 April 2018
0041-008X/ Published by Elsevier Inc.

Silver nanoparticles (AgNPs) are ENMs that are used in many consumer products and medical devices due to their highly antimicrobial properties (Woodrow Wilson International Center for Scholars, 2016). AgNPs act as antimicrobials by disrupting cellular proteins, enzymes, and DNA (Reidy et al., 2013). AgNPs have been shown to escape from functionalized materials and can enter water systems, air, dust and soil (Levard et al., 2012). Continued use of AgNPs in these and future applications increases the potential for human and environmental exposures.

Following *in vivo* oral and inhalation exposures to AgNPs, silver has been shown to translocate into the brain and activate local inflammatory responses in rats (Loeschner et al., 2011; Patchin et al., 2016; Yang et al., 2010). Tang et al. observed silver nanoparticles can cross the blood brain barrier both *in vivo* and *in vitro* (Tang et al., 2009, 2010). Silver has been detected in developing fetuses following oral and intravenous exposure to pregnant dams (Fennell et al., 2016). In addition, silver has been observed in brains of fetuses following oral administration of AgNPs to lactating dams (Morishita et al., 2016), indicating a potential for exposure to silver during critical periods of CNS development.

As their applications have continued to increase over time, AgNPs have been used in products including children's toys and clothing, as well as in products used by and marketed toward pregnant women (Quadros et al., 2013; Tulve et al., 2015; Woodrow Wilson International Center for Scholars, 2016). Use of AgNP-containing products during these sensitive periods of neurodevelopment creates a need for a more thorough understanding of whether exposure to AgNPs can disrupt the developing nervous system.

The goal of this study was to characterize the potential of AgNPs to interact with and disrupt the development of the CNS through use of a 3-dimensional organotypic *in vitro* micromass model. We determined whether developmental stage at the time of exposure and genetic differences has an impact on the extent of toxicity. In addition, we examine the role of AgNP size and coating on the relative toxicity of particles at these developmental stages.

Recent innovations in *in vitro* systems have led to the development of the micromass model. The high density, 3-dimensional micromass models (developed by Flint, 1983) enable investigators to study the formation of primary neural cell cultures through developmental stages of proliferation, adhesion, migration, and differentiation similar to *in vivo* development (Brown et al., 1995). Because of the 3-dimensional growth of micromass culture systems, stimulation with growth factors and differentiation-promoting factors is not required as development is driven by primarily on density. Micromass techniques have enhanced our understanding of neurodevelopmental systems by serving as a model for progression of *in vivo* neurodevelopment without the use of time intensive, costly *in vivo* studies (Whittaker et al., 1993; Sidhu et al., 2006; Whittaker and Faustman, 1991; Park et al., 2017).

Because of the unique characteristics of particles in liquid media, assessments in terms of concentration (by mass, surface area, or particle number) does not allow for direct comparison of different particles. Assessing effects in terms of dosimetry, or the amount of silver in or tightly associated with cells, creates a common denominator for comparing across particles, across culture systems, and to *in vivo* studies. As such, there is a need to assess silver dosimetry *in vitro* to appropriately estimate cytotoxic potential of AgNPs of different physicochemical properties on differing cell types (Wildt et al., 2016). To address this, we assessed cytotoxicity on our cultures *in vitro* by both nominal dose (μg/mL AgNP) and by dosimetric dose (ng Ag/mg protein) using inductively coupled plasma mass spectrometry (ICP-MS). Our AgNPs were manufactured using a gold (Au) core (Fennell et al., 2016; Munusamy et al., 2015; Shannahan et al., 2013), where Au served as a tracer to determine if Ag detected in cells resulted from nanoparticle uptake, silver dissolution, externally bound particles, or combinations of contributing factors. We compared effects observed in two strains of mouse to investigate genetic effects on AgNP neurodevelopmental toxicity.

## 2. Materials and methods

### 2.1. Silver nanoparticles

Citrate-stabilized 20 or 110 nm AgNPs (AgCitrate 20 and AgCitate 110) and Polyvinylpyrrolidone (PVP)- stabilized 110 nm AgNPs (AgPVP 110) were purchased from NanoComposix (San Diego, CA). All AgNPs contained a 7 nm diameter gold core. These particles were selected by the NIEHS Centers for Nanotechnology and Health Implications Research (NCNHIR) Consortium laboratories as common particles for investigation among Centers. Physicochemical properties of the AgNPs were provided by the manufacturer and other investigators (Fennell et al., 2016; Munusamy et al., 2015; Shannahan et al., 2013; Thomas et al., 2018). AgNPs were suspended in phosphate buffered saline (PBS) using water bath sonication and stored in 1 mg/mL stock solutions in the dark.

### 2.2. Culture system and conditions

We utilized previously optimized micromass culture methods described in Park et al. (2017). Briefly, we time mated both C57BL/6 and A/J mice and harvested primary midbrain cells from embryos of both sexes of C57BL/6 mice at gestation day 11 and A/J mice at gestation day 12. C57BL/6 and A/J mouse strains were chosen because they are frequently used in toxicological studies to examine differences in response due to different genetic backgrounds. These time points in gestation were confirmed to be equivalent between the two strains through confirmation of equal somite development. For each strain, embryonic midbrains from 3 dams (an average of 18 embryonic midbrains) were harvested and pooled for each biological replicate. We pooled midbrain cells of each strain into a single-cell suspension in media (DMEM/F-12, 10% FBS, 1% Penicillin/Streptomycin. 1% L-Glutamate) and plated them in 10 μL drops containing $5 \times 10^6$ cells on matrigel-coated (1:100 matrigel: PBS) 24-well (2 $cm^2$ well) Corning™ Primaria™ cell culture plates (Falcon, Corning, NY), maintaining separate cultures for each mouse strain. After plating, cultures were incubated at 37 °C for 1.5 h to allow cells to settle and attach to plates, after which 500 μL complete media was added to each well. Cultures received a full media change at 24 h after plating and subsequent half-media changes every other day until the time of AgNP exposure. The University of Washington Institutional Animal Care and Use Committee approved all experimental procedures used in this study.

Park et al. (2017) characterized this 3D organotypic micromass culture system in these two strains and showed neurodevelopmental growth patterns analogous to *in vivo* development. Briefly, cultures showed morphological changes (e.g., proliferation and migration) when observed with 400× magnification phase microscopy. Haematoxylin staining showed steady increases in neuronal differentiation over 22 days of the culture period in C57BL/6 and A/J systems, and that proliferation slowed after days *in vitro* (DIV) 6. Neurodevelopmental markers of proliferation (PCNA) showed proliferation peaked at DIV 4 and DIV 6 in both C57BL/6 and A/J strains. Markers of early differentiation (β-tubulin III and NeuN) peaked between DIV 6 and DIV 8, with markers of late differentiation (NMDAε1 and α-synuclein) peaking between DIV 8 and DIV 15 in both strains.

### 2.3. Exposure media preparation

Stock solutions of AgNPs in PBS (1 mg/mL) were suspended in complete culture media at concentrations of 6.25, 12.5, 25, and 50 μg/mL. ZnO served as a positive control at 50 μg/mL, and $TiO_2$ served as a negative control at 50 μg/mL. Stabilizer coating controls PVP 40kD (for PVP coated particles) and sodium citrate (for citrate- coated particles) were prepared in concentrations of 50 μg/mL and 100 μM, respectively.

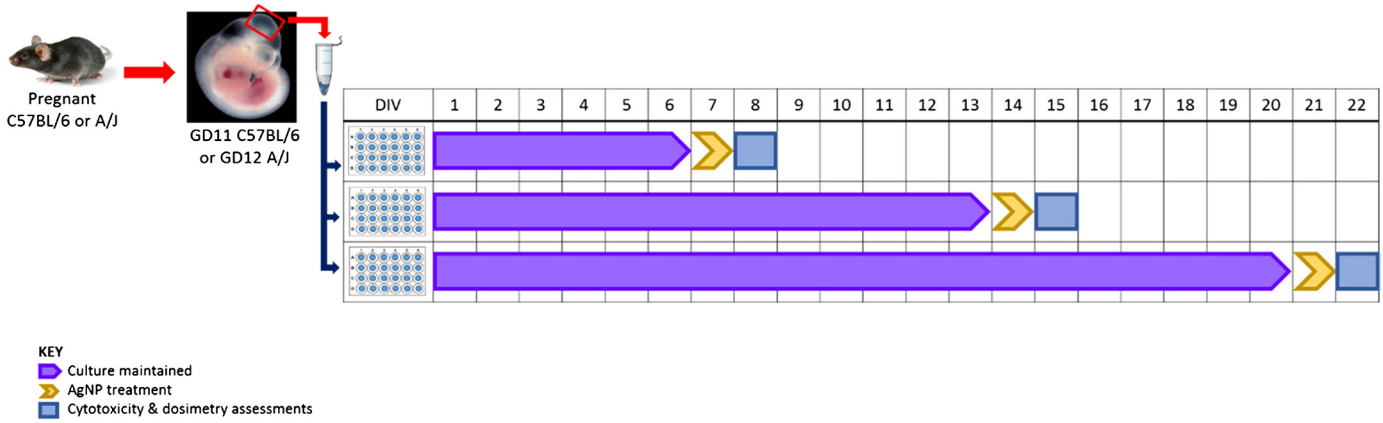


**Fig. 1.** Primary embryonic midbrains are harvested at gestation day 11 (C57BL/6) or gestation day 12 (A/J), brought into single cell suspension, and plated on 24-well plates. At days *in vitro* (DIV) 7, 14, and 21, cultures are exposed to various concentrations (μg/mL) of AgNPs, shown by the yellow arrows. After 24-hour incubation (at DIV 8, 15, and 22), cultures were harvested and assessed for uptake and toxicological endpoints. (For interpretation of the references to colour in this figure legend, the reader is referred to the web version of this article.)

These concentrations are equivalent to the amount of coatings present at the maximum concentrations that we have tested for AgNPs.

### 2.4. Silver nanoparticle exposure

Cell culture media was removed and 500 μL of AgNP exposure media at varying concentrations was pipetted in each well on 24-well plates and incubated at 37 °C for 24 h. We exposed micromass cultures to AgNPs of varying sizes and coating (AgCitrate 20, AgCitrate 110, AgPVP 110) at three separate time points, at DIV 7, 14, and 21. We assessed toxicity endpoints and dosimetry 24 h after the exposures, at DIV 8, 15, and 22, respectively, as shown in Fig. 1. Three time points (DIV 8, 15, and 22) were chosen based on the culture characterization study published by Park et al. (2017). Under control conditions, DIV8 is when proliferation markers (e.g. PCNA) have decreased and differentiation has been initiated (Park et al., 2017). DIV15 is during differentiation, where glutamate receptors (e.g. NMDAε1) and presynaptic markers (e.g. α-synuclein) showed the most significantly increased expressions (Park et al., 2017). DIV22 is when expression of differentiation markers (e.g. β-tubulin III, NMDAε1, and α-synuclein) decreased to the level similar to DIV1-4 (before the initiation of differentiation) (Park et al., 2017). For a given experiment, each treatment occurred once (not replenished), at one time point. All experimental conditions were performed in triplicate over three biological replicates.

### 2.5. Cytotoxicity assessment by lactate dehydrogenase (LDH) assay

Immediately following the 24-h exposures, we assessed LDH leakage in media as an indicator of cytotoxicity using Promega's Non-Radioactive Cytotoxicity Assay using the manufacturer's protocol (CytoTox 96® Non-Radioactive Cytotoxicity Kit; Promega, Madison, WI). Fifty microlitre of media was gently removed from each well (4 wells for each treatment group within a biological replicate; 3 biological replicates) and transferred to a 96 well plate. Care was taken to not disturb or take up any settled or floating particles as media was removed from each well. Assay reagent was added and allowed to react for 30 min before the stop solution was added and absorbance was measured colormetrically at 490 nm on a SpectraMax 190 plate reader (Molecular Devices, Sunnyvale, CA).

Data were normalized to a media blank and cytotoxicity was assessed as percent maximum LDH release (10% TritonX cell lysis solution provided in assay kit, incubated at 37 °C for 30 min) using the equation:

$$\%\text{LDH Max} = \frac{\text{Absorance of treated or control cells} - \text{Absorbance of blank media}}{\text{Absorbance of Maximum LDH} - \text{Absorbance of blank media}} \times 100\%$$

### 2.6. Dosimetry sample collection

Following the exposure and LDH assay, we removed the exposure media and washed the cells thoroughly to remove loosely associated and free AgNPs. We rinsed the cells 3× with 450 μL complete media, so as to not cause any changes in pH, temperature, or other culture conditions, and immediately removed the media following each rinse. Fresh media was used for each of the three rinses. After the rinses, we added a fresh 450 μL of media to each well and scraped cells from the plate. Complete removal of cells was confirmed through visual inspection of the well plate. We retained the scraped cell fractions for analysis by inductively coupled plasma mass spectrometry (ICP-MS) analysis of metals (Ag and Au) taken up or tightly associated with cells in culture. Triplicate samples of exposure media, rinses, and cells were combined for each treatment group within each biological replicate. Samples were stored in 15 mL polystyrene tubes (Corning Life Science, Corning, NY) and stored at 4 °C until time of ICP-MS analysis. Two biological replicates of cultures (cell fractions) exposed to 25 and 50 μg/mL of the three AgNP types as well as two coating controls were retained for determination of silver dosimetry.

Mass of Ag and Au in cell fractions were reported relative to total protein in each well. Total protein was determined in cell fractions of all dose groups following exposure by Bradford Protein Assay (Bio-Rad Laboratories, CA).

### 2.7. Determination of uptake

In order to determine whether toxicity observed following AgNP exposure resulted from uptake of dissolved Ag ions (dissolution in media) or from uptake and association of whole AgNPs, we utilized AgNPs that contained a small gold (Au) core (7 nm diameter core in all particles). We used ICP-MS to detect both Ag and Au in the exposure media (prior to exposure) and the cell fraction of cultures after 24-hour exposure, with the Au core serving as a tracer for whole or partially intact nanoparticles. We compared the concentrations of Ag to Au to determine if Ag in the cell fraction resulted from dissolution of Ag ions in media, from uptake or attachment of AgNPs, or from a combination of mechanisms.

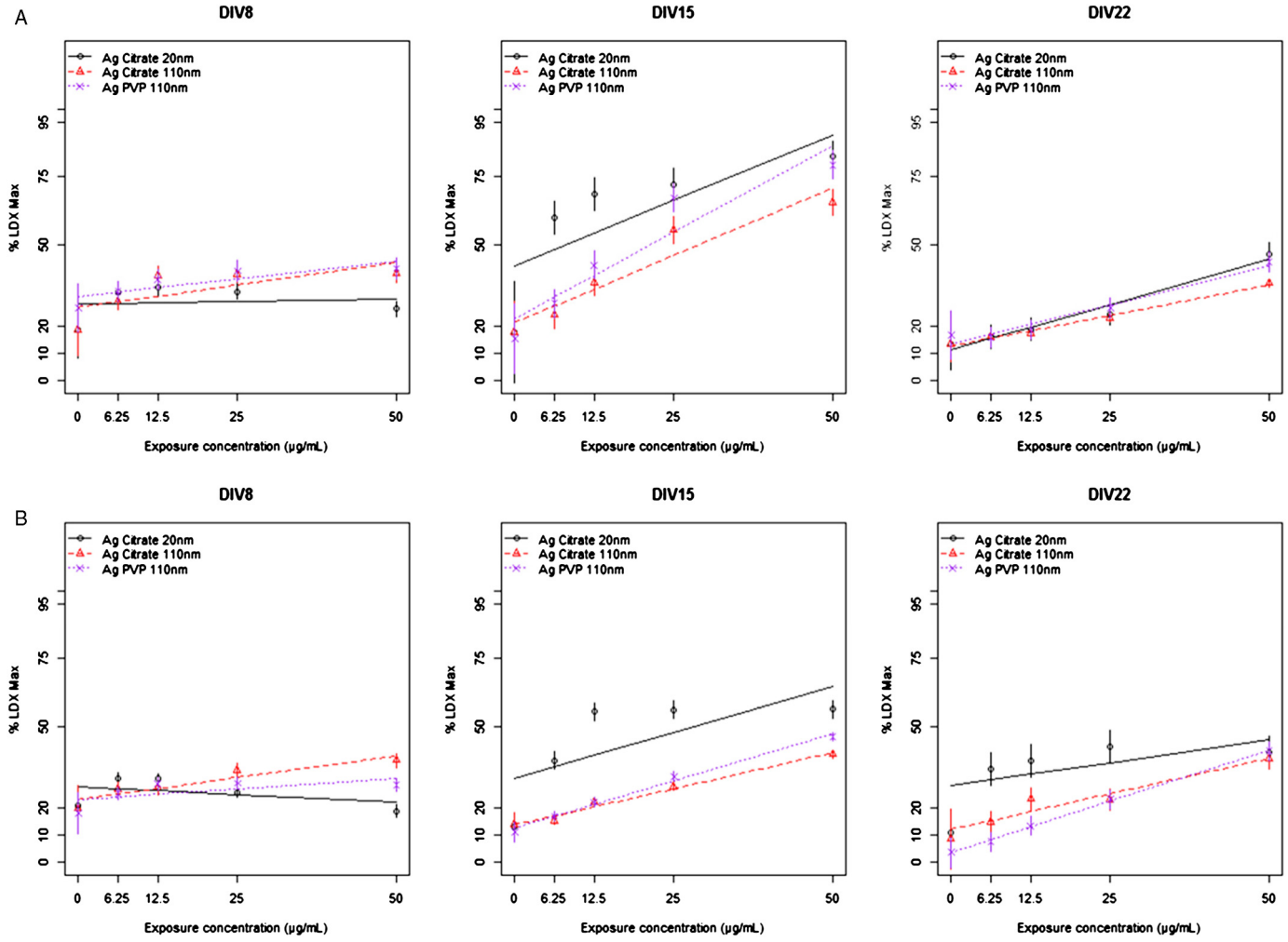


**Fig. 2.** Dose-response curves for effects of various silver nanoparticles. Dose-response curves for fetal (A) C57BL/6 and (B) A/J mouse midbrain cells after exposures to AgNPs. Of three different time points we have examined, 20 nm AgCitrate (black) showed the highest cytotoxicity at later time points (DIV 15 and 22) in both strains. At DIV 8, 110 nm particles (red and purple) lead to higher cytotoxicity in both strains. A significant difference between C57BL/6 and AJ was observed for 20 nm AgCitrate at DIV 22, for 110 nm AgCitrate at DIV 15, and for 110 nm AgPVP at DIV 15 and 22. Data points and lines were estimated from the mixed-effect model. (For interpretation of the references to colour in this figure legend, the reader is referred to the web version of this article.)

### 2.8. ICP-MS methods

The ICP-MS was conducted by University of Washington's Environmental Health Laboratory. Samples were prepared for inductively-coupled mass spectrometric (ICP-MS) analysis using open-vessel microwave-assisted digestion with mixed nitric and hydrochloric acids (trace-metal grade, Fisher) with Tb added as recovery standard (EPA, 2007). The microwave (MARS Xpress, CEM Inc.) program was temperature controlled: 800 W power (100%), 10 min ramp to 90 °C with a 20 min hold at final temperature. The digestate was brought to final volume with deionized water (≥18 Mohm) with final concentrations of 7% nitric acid, 2% hydrochloric acid, and 10 ng/mL Tb. The final HCl concentration was sufficient to stabilize $Ag^+$ as polychlorides at $Ag^+$ concentration ≤ 500 ng/mL.

Instrumental analysis was performed on an Agilent 7900 ICP-MS with SPS-4 autosampler and ISIS sample valve (Agilent Technologies, Santa Clara, CA). Acquisition (RF power, 1550 W; carrier gas flow, 1.03 L/min, spray chamber temp., 2 °C; helium (He) flow, 4.3 mL/min; nebulizer, Micromist) was done with He gas in the collision cell, which removes isobaric polyatomic interferences. Isotopes quantified were $^{197}Au$, $^{111}Cd$, and $^{107}Ag$ with $^{193}Ir$, $^{89}Y$, and $^{159}Tb$ used as internal stable isotope standards. Calibrants were made from commercial stock solutions (Aristar BDH) with independent check standard from second vendor (Ultra Scientific). Stock solutions were certified reference materials (ISO Guide 34). Continuing calibration verification was performed approximately every 30 samples. Data was corrected for process blanks.

### 2.9. Statistical analysis

We used R statistical software (The R Core Team, 2013) to create mixed effects dose-response regression model curves to relate cytotoxicity to the fixed effects of the three types of AgNPs (AgCitrate 20 nm, AgCitrate 110 nm, and AgPVP 110 nm) at three developmental stages (DIV 8, 15, and 22) in two mouse strains (A/J and C57BL/6) based upon nominal dosses or Ag dosimetry. Within the mixed effects model, the random effect was defined as each biological replicate to account for any variability between different culture preps. To test differences between dose-response regression curves we first stratified by two of the fixed effects and then tested the effect of the third fixed effect on the dose response slopes in the mixed effect model. For example, in the results sections on "Dose response effects" we stratified by developmental stages (DIV 8, 15, 22) and mouse strain (A/J and C57BL/6) then tested the slopes for each particle type (AgCitrate 20 nm, AgCitrate 110 nm, and AgPVP 110 nm). Using this stratification, we performed post-hoc tests in the "Particle size effects" and "Particle

coating effects" sections. In the sections on "Developmental stages" we stratified by type of nanoparticle and mouse strain and then used post hoc tests to determine significant differences between slopes for developmental stages. To test the differences between genetic strains we stratified by particle type and developmental stage.

We modeled Ag dosimetry in cultures after 24 h of exposure to each particle type at nominal doses of 0 lμg/mL, 25 μg/mL and 50 μg/mL using a mixed effects model with biological replicate as the random effect. We used the dosimetry mixed effects regression model to determine Ag concentration per mg protein at each nominal exposure concentration. We then modeled the cytotoxicity dose response as a function of the dosimetry determined Ag concentration per mg protein using a mixed effects model, again with the biological replicate serving as the random effect.

## 3. Results

### 3.1. AgNP cytotoxicity by nominal dose

To assess the effects of dose, timing of exposure, size, and coating of particles on our developing culture systems, we created a mixed effect dose-response model of the three species of AgNPs at three time points in both the C57BL/6 and A/J strains. Results from coating controls were shown as 0 μg/mL.

### 3.2. Dose response effects by nominal dose in C57BL/6

Regression models showed a significant positive dose-response effect from exposure to Ag Citrate 20 nm at DIV 15 ($p < 0.001$) and DIV 22 ($p < 0.001$), but did not show a significant dose response at DIV 8 (Fig. 2A, left panel). Ag Citrate 110 nm (Fig. 2A, middle panel) showed a significant dose response effect at all time points ($p < 0.001$). Ag PVP 110 nm (Fig. 2A, right panel) showed a significant dose response at all time points ($p < 0.001$).

### 3.3. Dose response effects by nominal dose in A/J

When cytotoxicity was measured at DIV 8, 15, and 22 after 24-hour exposure to 20 nm AgCitrate, 110 nm AgCitrate, or 110 nm AgPVP, all AgNPs showed a significant dose response relationship at all time points in the A/J strain (Fig. 2B). For 20 nm AgCitrate, a significantly negative dose response relationship was observed at DIV 8 ($p < 0.05$) while significantly positive relationships were found at DIV 15 ($p < 0.001$) and DIV 22 ($p < 0.01$). Please note that although a significant negative relationship was seen for DIV 8 at 20 nm AgCitrate, the actual changes in cytotoxicity represented over these concentrations was < 10%. Both 110 nm particles (citrate and PVP coated) illustrated a significant dose response relationship at all time ($p < 0.001$ for both particles at all time points).

### 3.4. Developmental stage at time of exposure by nominal dose in C57BL/6

We found that developmental time of exposure has a significant effect on the extent of cytotoxicity among all time points (Fig. 2A). Post-hoc tests showed that overall exposures at DIV 15 showed the greatest cytotoxic effect in all particles ($p < 0.001$). Cultures were more sensitive to AgCitrate 20 particles (Fig. 2A) at DIV 15 and DIV 22 compared to DIV 8 ($p < 0.001$ and $p < 0.01$, respectively). AgCitrate 110 (Fig. 2A) showed the greatest cytotoxic effect at DIV 15 compared to DIV 8 and DIV 22 ($p < 0.001$ and $p < 0.001$). When exposed to AgPVP 110 (Fig. 2A), cultures showed significantly greater cytotoxicity at DIV 15 compared to DIV 8 and DIV 22 ($p < 0.001$ and $p < 0.001$). In addition, cultures were more sensitive to AgPVP 110 at DIV 22 compared to DIV 8 ($p < 0.05$).

### 3.5. Developmental stage at time of exposure by nominal dose in A/J

The embryonic A/J mouse micromass system illustrated that developmental stages at time of exposure affected cytotoxic responses to AgNPs. A greater cytotoxicity response was observed at DIV 15 and 22 than DIV 8 ($p < 0.001$ and $p < 0.05$) after exposures to 20 nm AgCitrate. For 110 nm AgPVP, the cytotoxicity response at DIV 15 and 22 was significantly different from the one at DIV 8 ($p < 0.001$ and $p < 0.001$). No effect of time of exposure on toxicity was found for 110 nm AgCitrate.

### 3.6. Particle size effects by nominal dose in C57BL/6

To investigate the effect of particle size on cytotoxicity, we compared AgCitrate 110 and AgCitrate 20 using a post hoc test at each time point. At DIV 8 (Fig. 2A, left panel) we observed a greater effect on cytotoxicity from the 110 nm particle compared to the 20 nm particle ($p < 0.01$). At DIV 22 (right panel) we observed greater effect after exposure to the 20 nm particle compared to the 110 nm particle ($p < 0.05$). No effect of size on toxicity was observed at DIV 15 (middle panel).

### 3.7. Particle size effects by nominal dose in A/J

The A/J mouse midbrain micromass system revealed effects of particle sizes on cytotoxicity at DIV 8. At DIV 8, 110 nm AgCitrate induced greater cytotoxicity compared to 20 nm AgCitrate ($p < 0.001$) (Fig. 2B, left panel). Particle size did not significantly impact cytotoxicity at DIV 15 (middle panel) and DIV 22 (right panel).

### 3.8. Particle coating effects by nominal dose in C57BL/6

We investigated the effect of coating on cytotoxicity by comparing AgCitrate 110 and AgPVP 110 using a post hoc test (Fig. 2A). We observed a significant effect of coating on cytotoxicity at DIV 15 ($p < 0.05$).

### 3.9. Particle coating effects by nominal dose in A/J

When differences in response due to particle coating was examined, a significant effect of coating (citrate vs. PVP coating) on cytotoxicity at all time points ($p < 0.05$ for DIV 8 and 22; $p < 0.001$ for DIV 15) in the A/J strain (Fig. 2B).

### 3.10. Dosimetry results in C57BL/6 and A/J

To determine Ag dosimetry (uptake and tightly associated Ag) following 24-hour AgNP exposure, we harvested cell cultures and performed ICP-MS analysis for metals. Mass of Ag was reported relative to total protein in cell cultures after exposure. We found Ag in cell fractions increased linearly with exposure concentration for all particles at all time points in both strains (Fig. 3). Similar amounts of Ag were observed to be associated with cells at all time points for 20 nm AgCitrate particles. The 110 nm particles (both citrate and PVP coated) showed similar amounts of silver at DIV 15 and DIV 22, but showed significantly less silver uptake at DIV 8 (middle and right panels). The larger (110 nm) AgNPs resulted in greater amounts of Ag in cultures compared to smaller particles at all time points (Fig. 4B). No difference in uptake was observed between different coatings.

### 3.11. Dose-response effects by dosimetry

We assessed the effects of dose, developmental stage, size, and coating of particles on cytotoxicity in developing cultures using a mixed effects model by dosimetric dose (μg Ag/mg protein). Developmental stage at time of exposure was compared within each particle and effects

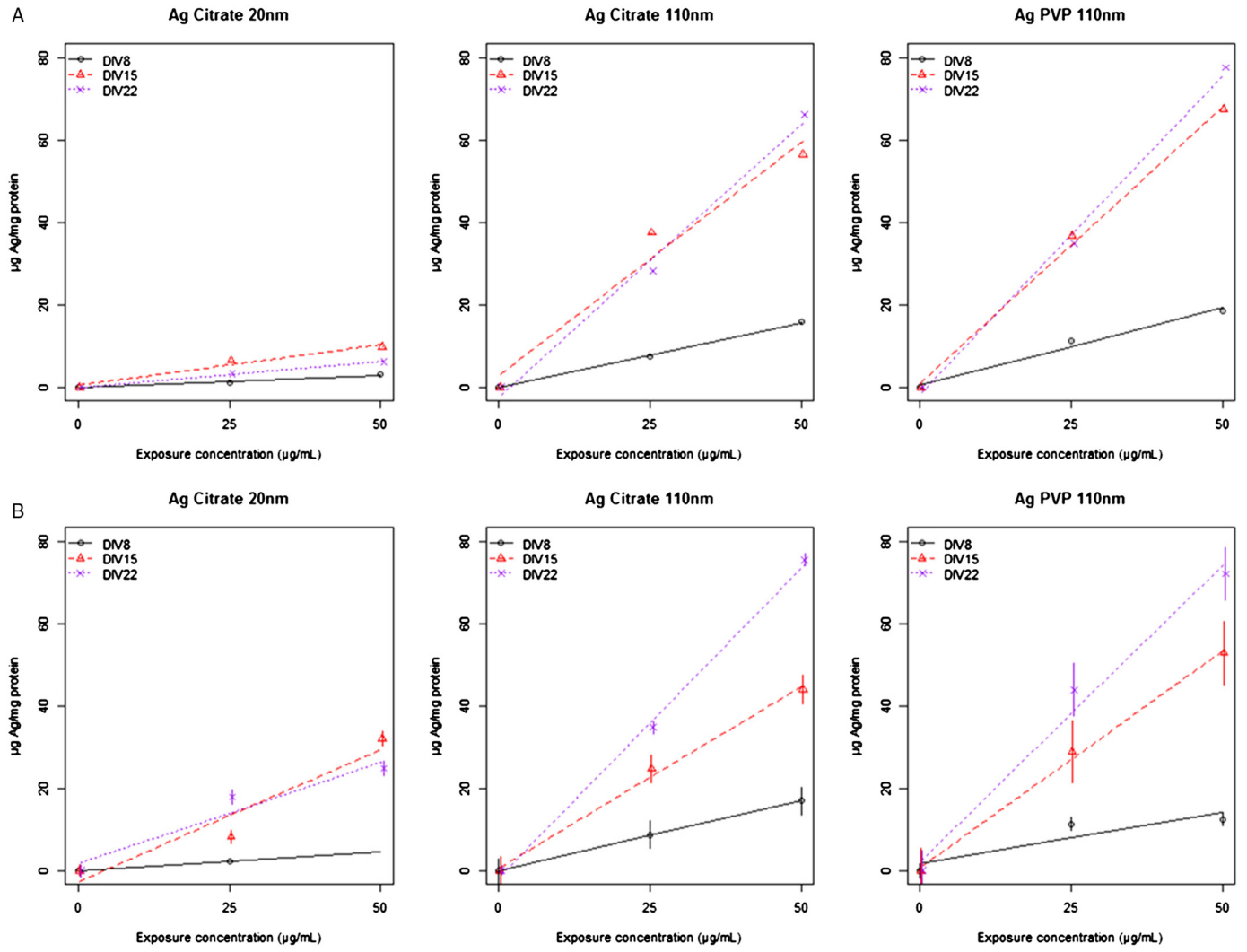


**Fig. 3.** Dosimetry of Ag (µg Ag/mg protein) in cells after 24 h exposure to three particles. Ag dosimetry increased linearly in all particles at all days in both the (A) C57BL/6 and (B) A/J strains.

of particle size and coating was compared within each time point (Fig. 4).

### 3.12. Dose response effects by dosimetry in C57BL/6

We used regression in mixed effects models to determine the significance of dose-responses after exposure to AgNPs by Ag dosimetry. We observed a significant dose response in all particles at all time points ($p < 0.001$), with the exception of 20 nm AgCitrate at DIV 8 in the C57BL/6 strain (Fig. 4A).

### 3.13. Dose response effects by dosimetry in A/J

AgNPs taken up by the embryonic A/J mouse midbrain cells were measured and were used to adjust for cytotoxic responses. After dosimetry adjustments, a significant dose response relationship was found in all particles at all time points ($p < 0.05$ for 110 nm AgCitrate at DIV 8; $p < 0.01$ for 20 nm AgCitrate at DIV 22, 110 nm AgCitrate at DIV 15 and 22, and 110 nm AgPVP at DIV 15 and 22), except for 20 nm AgCitrate at DIV 8 and DIV 15 and for 110 nm AgPVP at DIV 8 (Fig. 4B).

### 3.14. Effect of developmental stage at time of exposure by dosimetry in C57BL/6

Cultures were more sensitive to exposure to the 110 nm AgPVP particle at DIV 15 compared to DIV 22 ($p < 0.001$) in the C57BL/6 strain (Fig. 4A). Differences in timing of exposure were not significant for the 20 nm Citrate particle.

### 3.15. Effect of developmental stage at time of exposure by dosimetry in A/J

Exposures to 20 nm AgCitrate showed a significantly greater dosimetry adjusted cytotoxic response at DIV 15 than DIV 22 ($p < 0.05$) in the A/J strain (Fig. 4B). Similar result was found for 110 nm AgCitrate where cytotoxicity adjusted by dosimetry was significantly greater at DIV 15 when compared to that at DIV 22 ($p < 0.001$). No significant effects of developmental stage at time of exposure were observed for 110 nm AgPVP.

### 3.16. Particle size effects by dosimetry in C57BL/6

When comparing differences in effect of particles (Fig. 4A), we found AgCitrate 20 nm particles were significantly more toxic compared to AgCitrate 110 nm particles at DIV 15 ($p < 0.001$) and at DIV 22 ($p < 0.001$). No effect of particle size was seen at DIV 8

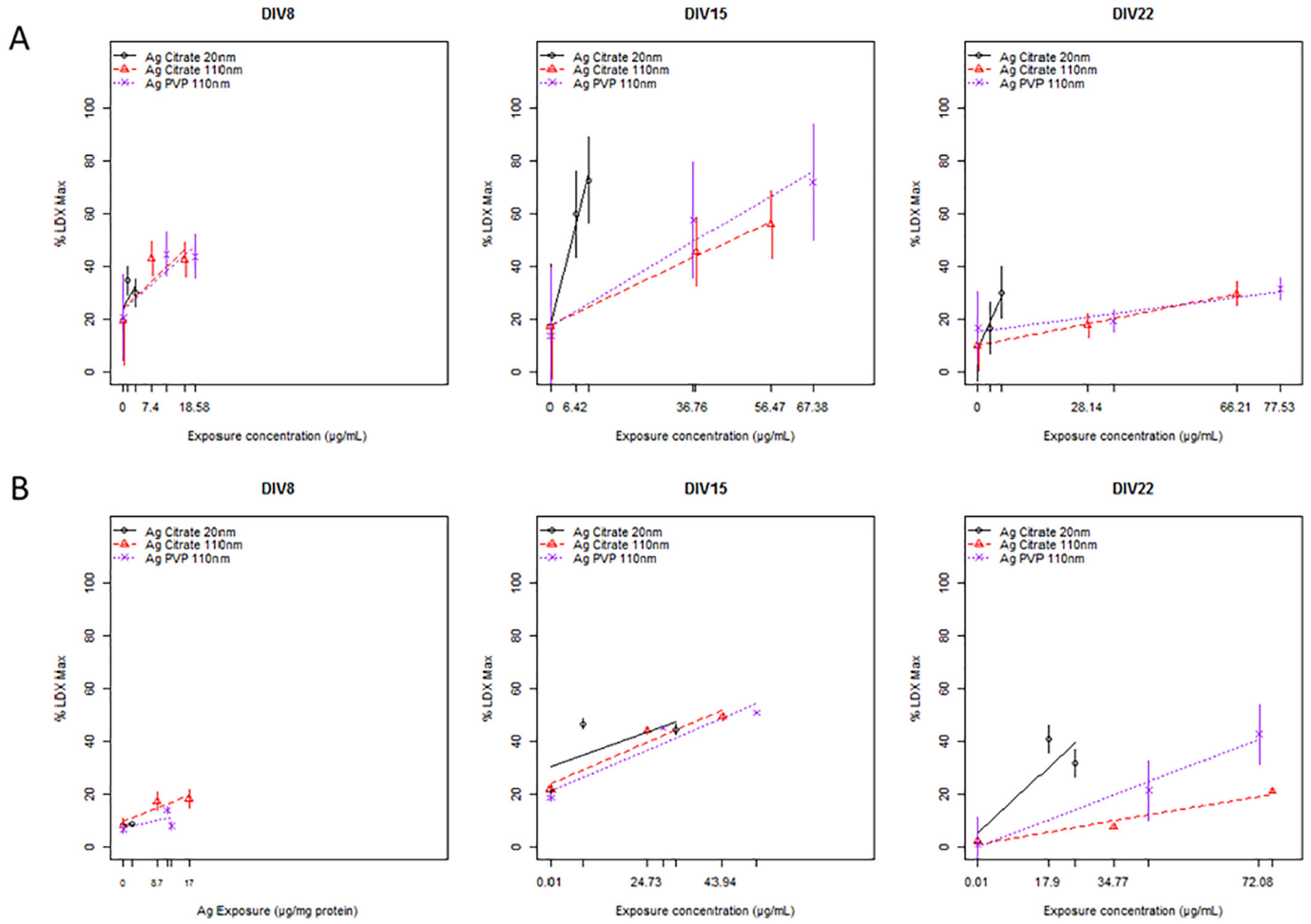


**Fig. 4.** Dosimetry adjusted dose-response curves for effects of different AgNPs. Dosimetry-response curves for fetal (A) C57BL/6 and (B) A/J mouse midbrain cells after exposures to three different AgNPs. Even after adjusting for the amount of AgNPs associated with cells, cells were most susceptible to 20 nm particles than 110 nm particles for both strains of mouse. Data points and lines were estimated from the mixed-effect model.

($p > 0.05$).

### 3.17. Particle size effects by dosimetry in A/J

Particle size did not affect responses to 20 nm and 110 nm AgCitrate exposures on embryonic A/J mouse midbrain cells at DIV 8 ($p > 0.05$) and 15 ($p > 0.05$); however, 20 nm AgCitrate resulted significantly greater cytotoxicity compared to 110 nm AgCitrate at DIV 22 ($p < 0.01$).

### 3.18. Particle coating effects by dosimetry in C57BL/6

No differences in the effect of coating were observed between citrate and PVP-coated particles at any time points ($p > 0.05$) in the C57BL/6 strain.

### 3.19. Particle coating effects by dosimetry in A/J

In the A/J strain, particle coating was a significant contributor on cytotoxicity of AgNPs with citrate and PVP-coating at DIV 22 ($p < 0.05$), but at not DIV 8 ($p > 0.05$) and 15 ($p > 0.05$).

### 3.20. Effects of genetic strain on cytotoxicity with and without dosimetry adjustment

The potential contribution of genetics in response to AgNP exposures were examined by comparing embryonic C57BL/6 and A/J mouse midbrain cells. Prior to dosimetry adjustments, a significant strain difference was observed at DIV 15 for 110 nm AgCitrate and AgPVP ($p < 0.001$) (Supplemental Table 1). Strain differences were also found at DIV 22 after exposures to 20 nm AgCitrate ($p < 0.05$) and 110 nm AgPVP ($p < 0.05$) (Supplemental Table 1). After adjusting cytotoxicity using dosimetry data, C57BL/6 and A/J mouse strains illustrated significant differences in dosimetry adjusted cytotoxicity for 20 nm AgCitrate at DIV 15 ($p < 0.01$) and for 110 nm AgPVP at DIV 22 ($p < 0.05$) (Supplemental Table 2).

### 3.21. Determination of dissolution activity and particle uptake in C57BL/6 and A/J

We performed an analysis of Ag and Au in both exposure media (prior to exposure) and in cell fractions after exposure to determine the difference in proportions of Ag and Au for each particle at 25 and 50 µg/mL. Time points (DIVs) were not separated in order to investigate an overall trend for dissolution. We observed a greater amount of Au relative to Ag in 20 nm particles (gray and black) compared to 110 nm particles (blue, red, pink). We did not observe a significant difference in relative amounts of Ag and Au between exposure media (triangles) and cell fractions (circles) for any particle type in the C57BL/6 strain ($p > 0.05$) (Fig. 5). However, we see in the A/J strain changes in relative amounts of Ag and Au between exposure medium and cell fractions for all particle types (Fig. 6). These observations require further

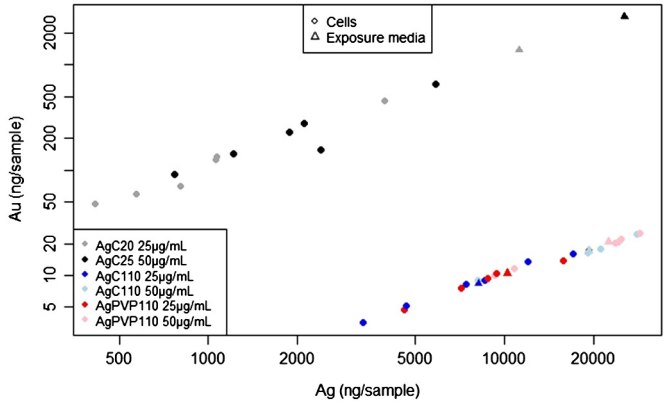


**Fig. 5.** Ag and Au in C57BL/6 cell fraction (circles) at all time points following 24 h AgNP exposure and exposure media prior to exposure (triangles). A smaller ratio of Ag to Au was observed in 20 nm particles (gray and black). No difference in relative amounts of Au and Ag was observed between exposure media prior to exposures and cell fractions following exposure to all particles.

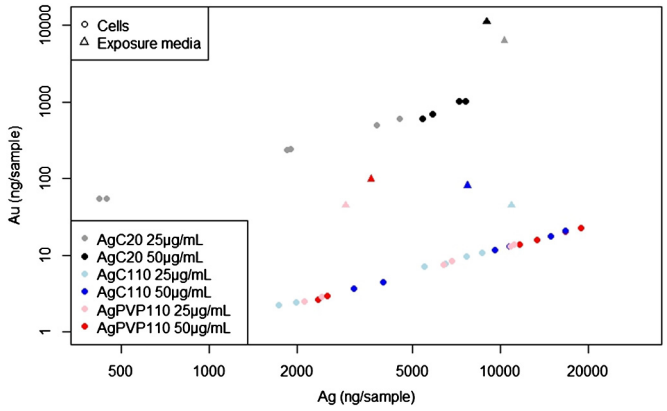


**Fig. 6.** Ag and Au in A/J cell fraction (circles) at all time points following 24 h AgNP exposure and exposure media prior to exposure (triangles). A smaller ratio of Ag to Au is observed in 20 nm particles (gray and black). A difference in relative amounts of Au and Ag is observed between exposure media prior to exposures and cell fractions following exposure in all particle sizes and coatings.

follow up to understand the potential for strain differences in dissolution and particle uptake on toxicity of silver nanoparticles.

## 4. Discussion

There is a need to assess the potential for environmental agents to act as neurodevelopmental toxicants. In this study, we utilized a 3-dimensional organotypic mouse midbrain model to assess the sensitivity of developing primary mouse neural cultures to AgNPs. We investigated the effect of developmental stage at time of exposure as well as the contribution of AgNP size and coating to toxicity. In addition, we measured the contributions of dissolved Ag and intact AgNPs to observed toxicity.

*In vitro* models provide several advantages over the use of *in vivo* toxicity assessments as they utilize significantly fewer animals, can assess multiple endpoints simultaneously, allow for rapid, high throughput assessments, and often cost far less than animal toxicity studies. These attractive qualities of assessing toxicity using *in vitro* models become even more powerful and necessary to keep pace with the accelerating rate of scientific and technological advancements in chemical and manufactured materials. We utilized an innovative method for assessing neurodevelopmental effects through our 3-dimensional micromass model that has been shown to grow and develop without the addition of growth factors or differentiation promoting factors (Park et al., 2017). The ability to study neurodevelopment *in vitro* without use of these factors is critical for neurodevelopmental toxicity studies as these growth factors may mask sensitivity of effects. In addition, many of these factors may be retinoic acid-based (Maden, 2007), and may sensitize neural cultures to developmental disruption as retinoic acid is a well characterized teratogen (Lammer et al., 1985). The European Centre for the Evaluation of Alternative Methods (ECVAM) has supported the use of micromass cultures as a standard alternative developmental toxicity method in an effort to reduce the number of animals used in toxicity studies (ECVAM, 2001).

Park et al. (2017) developed and thoroughly characterized a micromass culture system from primary embryonic mouse midbrains. A mouse culture system allows for higher throughput with development occurring in a shorted period of time compared to rat and other mammalian models. In addition, the availability of many inbred genetic strains of mouse allows for the comparison of results across strains for insights on genetic influences of variability in response. This is especially useful in comparison across the Collaborative Cross mouse strains which include both the C57BL/6 and A/J strains used in this study (Churchill et al., 2004). Neurodevelopmental processes are largely conserved across mammalian species and as such, a mouse embryonic midbrain cell model may serve as an effective tool to assess the potential for AgNPs to cause neurodevelopmental toxicity in humans as we explore results for mice model reflecting human variability.

AgNPs utilized in these experiments were manufactured on an Au core (7 nm), allowing us to collocate Ag and Au and to determine whether whole nanoparticles or Ag in media contributed to cytotoxicity observed. We compared the concentrations of Ag to Au in exposure media (before exposure) and in cell fractions (after 24 h AgNP exposure) and hypothesized that a larger relative ratio of Ag to Au in cell cultures after exposure would suggest that Ag may have preceded dissolution from Au core in media. However, we did not observe a significant difference between the relative ratios of Ag and Au in exposure media compared to C57BL/6 mouse cells after exposure to any of the three particles investigated. This suggests that dissolution of particles in media is not a major contributing factor to cytotoxicity observed in this strain, and that particles are eliciting cytotoxic effects in these cultures are either taken up by cells or are eliciting effects while associated with Au. Interestingly, the A/J strain showed differences and more variabilities in the relative ratios of Ag and Au between exposure media and cells post exposure. It is possible that this effect is due to differences in cellular response between strains as Scoville et al. (2017) observed greater neutrophil response in A/J strain compared to C57BL/6 strain after exposure to AgNPs. These differences in cellular response between strains after AgNP exposure may be related to the observed differences between strains in the apparent cellular uptake of AgNPs in the present study.

There has been a great deal of discussion as to whether toxic effects from AgNPs observed *in vitro* and *in vivo* are due to cellular uptake of particles or from dissolution of AgNPs into free Ag ions in media.

Dissolution of AgNPs has been observed to occur both *in vitro* and *in vivo*. The rate of dissolution has been shown to depend on particle size, pH and temperature of the environment, other ions present in media, aggregation state, and incubation time (Leo et al., 2013; Loeschner et al., 2011; Stebounova et al., 2011). Smaller nanoparticles have been observed to dissolve faster due to their high surface to volume ratio. Ma et al. (2012) found the dissolution of AgNPs to range from 1% for 80 nm particles to 60% for 5 nm particles at pH 8 during three and two months of incubation, respectively. Because smaller AgNPs have greater surface area per mass compared to larger particles, a higher degree of dissolution may occur, leading to a greater number of free Ag ions and greater toxic potential. Surface area of particles has been suggested to be the greatest predictor of AgNP toxicity compared to other physicochemical characteristics such as mass (Braakhuis et al., 2016; Oberdorster et al., 2005). The smaller sized nanoparticles have been

shown to have a higher dissolution rate and lower biodurability and thus greater potential to cause pathogenicity (Utembe et al., 2015). In addition, protein in serum or culture media can form a protein corona around silver particles, stabilizing them and reducing dissolution rate (Duran et al., 2015; Shannahan et al., 2013).

We observed significantly greater effects on cytotoxicity when exposures occurred at DIV 15 compared to DIV 8 and 22 in both C57BL/6 and A/J strains. This effect was consistent in both nominal dose and dosimetric dose response assessments, despite an equivalent amount of Ag associated with cells at DIV 15 and DIV 22.

Park et al., 2017 observed that these same micromass cultures show peaks of both early and late phase differentiation markers (β-tubulin III, NeuN, α-synuclein, and NMDAε1) at DIV 15 compared to other time points. This suggested that neural differentiation may be the "critical windows of susceptibility" to AgNPs like many other toxicants (Rodier, 1994, 1995). Our findings of neural culture sensitivity during differentiation have also been observed in other *in vitro* neurodevelopment models. Greater sensitivity to metals has been shown during neural differentiation stages of development after exposure to manganese (Hernandez et al., 2011), lead (Bull et al., 1983; Silbergeld, 1992; Deng et al., 2001), and methylmercury (Barone Jr et al., 1998).

Differentiation into specialized cell types may contribute to the increased sensitivity of cultures at later time points. The midbrain contains the greatest amount of dopaminergic neurons in the brain and they first begin to appear at embryonic day 10.5 (Maxwell and Li, 2005)- roughly the time when our cultures are harvested and plated. Early dopaminergic neurons proceed through several stages of development and become functionally mature several days later which may coincide with DIV 15 in these cultures (Abeliovich and Hammond, 2007). Metals have been shown to accumulate in dopaminergic neurons (Robison et al., 2015). Alternatively, increased uptake and cytotoxicity of AgNPs at DIV 15 may be due to differentiation into less specialized neurons, however the potential for $Ag^+$ to utilize $Na^+$ channels may lead to increased uptake of Ag and a disruption of ion flow (Bury and Wood, 1999). Alternatively, microglia and other glial cell types may develop just prior to DIV 15, leading to the increased update of particles observed.

When compared by dosimetry, we found that the smaller particle (AgCitrate 20 nm) had greater cytotoxic effects than larger particles at DIV 15 and DIV 22 in both strains. This effect was observed despite significantly less Ag (and total Ag + Au) in cell cultures after exposure to 20 nm particles. The apparent absence of dissolution in media from either size particle (no difference in Ag:Au between media and cells), despite significant differences in particle size on toxicity may be explained by dissolution occurring primarily in lysosomes. As nanoparticles are taken up into cells, autophagosomes form around particles and other damaged cellular components. Lysosomes then fuse with autophagosomes and hydrolytic enzymes degrade its contents. Because lysosomes are more acidic (pH 5–6) than cytosol and other cellular components, the acidic environment may result in enhanced AgNP dissolution. Because smaller particles have greater surface area compared to larger particles, this may result in a heightened level of dissolution. As such, more dissolution may occur with smaller particles, leading to greater lysosomal dysfunction and cell death. Stern et al. (2012) and Ma et al. (2012) found lysosomes play a large role in cytotoxicity and has been proposed to be a major mechanism in nanoparticle toxicity.

Alternatively, it is possible that the 20 nm AgNPs are undergoing so much dissolution in media that the Au core becomes exposed and also undergoes dissolution and uptake into cells. This would also result in the observed lack of change in proportion of Ag to Au for 20 nm particles. Munusamy et al. (2015) found 20 nm AgNPs containing an Au core had much more rapid dissolution rate in media (approximately 50% particle mass dissolved after 24 h) compared to 110 nm AgNPs with an Au core (approx. 20% particle mass dissolved after 24 h). This would not, however explain the lack of change in relative amounts of Ag to Au in 110 nm particles before and after exposure. It is possible that cytotoxicity may be occurring through differing mechanisms of delivery of metals to cells between particle sizes, where 110 nm particles elicit effects by associating with outer layers of cell membranes or are taken up into cells as mostly undissolved particles. This may explain why much greater amounts of Ag is found in cell fractions following exposure to 110 nm cells.

Coatings such as citrate and polyvinyprridolone (PVP) work to stabilize silver nanoparticles by reducing aggregation and agglomeration and controlling ion release from particles. In our study, we found significant differences between PVP- and citrate-coated particles of the same size prior to dosimetry analysis. Effects of coating on cytotoxicity, however, disappeared upon adjustment with dosimetry data in the C57BL/6 strain, but the coating effect remained in the A/J strain at DIV 22. Interestingly, PVP has been shown to complex with releasing $Ag^+$ ions and has been shown to reduce cytotoxic effects of AgNPs compared to the same sized citrate-coated particles, however we did not observe this effect in our study (Wang et al., 2014).

When assessing differences in AgNP effects between strains, we observed differences in response to AgNP exposures with the 20 nm AgCitrate particles at DIV 22. Effect of strain was also observed for 110 nm AgCitrate at DIV 15 and for 110 nm AgPVP at DIV 15 and 22. This effect remained in 20 nm AgCitrate at DIV 15 and 110 nm AgPVP at DIV 22 after adjusted with dosimetry, suggesting that dosimetry is critical when investigating effects of AgNPs in *in vitro* culture systems. In addition to significant differences in cytotoxic response observed between the two strains investigated, strain differences in dissolution of particles brings to light the potential for genetic effects on uptake and association of AgNPs. These effects observed *in vitro* may potentially occur *in vivo*. These observations may also be considered for other forms of semi-soluble inorganic nanoparticles.

The present study provides valuable insight on the potential for AgNPs to interact with and disrupt developing neural cultures, however several limitations of this work have been identified. While our methods were designed to prevent large amounts of aggregation and agglomeration of particles in media, we did not measure AgNP aggregation or agglomeration in exposure solution prior to exposures. This could potentially result in reduced delivery of AgNPs to cultures and may affect uptake and cytotoxicity. As such, the differences in behavior of different sized particles in liquid media may also affect delivery to cultures, and may lead to differences in toxic effects. We addressed some of these potential differences in delivery by assessing dosimetry after exposures to compare between particles however, the translation of particle delivery to tissue *in vivo* may be quite different. We investigated differences in concentrations of Ag to Au before and after exposures to determine the extent by which dissolution of AgNPs in culture media contributes to cytotoxicity. This analysis showed that there was no significant change in ratios in any of the three particles investigated. However, our methods did not allow for the determination of whether complete dissolution of particles occurred in media, which could also result in the lack of change in ratio of metals. Visualization of cells after exposure by electron microscopy and measurement of particles associated with cells may better inform whether uptake of whole particles is occurring.

In summary, we have shown our 3-dimensional developing primary midbrain cultures are sensitive to AgNPs. Cultures were more sensitive to AgNP exposures at differentiation stages of development, with greater uptake of particles occurring at later time points. Cultures were more sensitive to smaller sized AgNPs, despite less overall uptake of Ag compared to larger particles. Similar cytotoxic effects were observed in both the C57BL/6 and A/J strains. Despite this, we found differences in dissolution and uptake of dissolved silver and whole AgNPs between the two strains, suggesting genetic differences in uptake mechanisms. Future work may investigate markers for dopaminergic neurons or microglia in these cultures to better inform the role of cell type differentiation and mechanisms of uptake and sensitivity observed in

cultures at later time points.

## Conflict of interest statement

None of the authors have any conflicts of interest

## Acknowledgements

We thank University of Washington's undergraduate research assistants for their technical support. This work was supported by the National Institutes of Health (National Institute of Environmental Health Sciences NIH/NIEHS) grants U19ES019545, P30ES007033, and US Environmental Protection Agency (EPA) grant RD83573801 and done in collaboration with NCNHIR Consortium.

## Appendix A. Supplementary data

Supplementary data to this article can be found online at https://doi.org/10.1016/j.taap.2018.04.017.

## References

Abeliovich, A., Hammond, R., 2007. Midbrain dopamine neuron differentiation: factors and fates. Dev. Biol. 304, 447–454. doi:S0012-1606(07)00065-6 [pii]. https://doi.org/10.1016/j.ydbio.2007.01.032.

Barone Jr., S., Haykal-Coates, N., Parran, D.K., et al., 1998. Gestational exposure to methylmercury alters the developmental pattern of trk-like immunoreactivity in the rat brain and results in cortical dysmorphology. Brain Res. Dev. Brain Res. 109, 13–31.

Braakhuis, H.M., Cassee, F.R., Fokkens, P.H., et al., 2016. Identification of the appropriate dose metric for pulmonary inflammation of silver nanoparticles in an inhalation toxicity study. Nanotoxicology 10, 63–73. http://dx.doi.org/10.3109/17435390.2015.1012184.

Brown, S., Bechter, Flint, Freeman, Jelinek, Koch, Nau, Newall, Palmer, Renault, Repetto, Vogel, Wiger, 1995. Screening chemicals for reproductive toxicity: the current alternatives. ATLA 23, 868–882.

Bull, R.J., McCauley, P.T., Taylor, D.H., et al., 1983. The effects of lead on the developing central nervous system of the rat. Neurotoxicology 4, 1–17.

Bury, N.R., Wood, C.M., 1999. Mechanism of branchial apical silver uptake by rainbow trout is via the proton-coupled Na(+) channel. Am. J. Phys. 277, R1385–1391.

Churchill, G.A., Airey, D.C., Allayee, H., et al., 2004. The collaborative cross, a community resource for the genetic analysis of complex traits. Nat. Genet. 36, 1133–1137. doi:ng1104-1133 [pii]. https://doi.org/10.1038/ng1104-1133.

Deng, W., McKinnon, R.D., Poretz, R.D., 2001. Lead exposure delays the differentiation of oligodendroglial progenitors in vitro. Toxicol. Appl. Pharmacol. 174, 235–244. http://dx.doi.org/10.1006/taap.2001.9219.

Duran, N., Silveira, C.P., Duran, M., et al., 2015. Silver nanoparticle protein corona and toxicity: a mini-review. J Nanobiotechnology 13, 55. http://dx.doi.org/10.1186/s12951-015-0114-4.

EPA, 2007. Method 3051- A Microwave Assisted Acid Digestion of Sediments, Sludges, Soils, and Oils.

Fennell, T.R., Mortensen, N.P., Black, S.R., et al., 2016. Disposition of intravenously or orally administered silver nanoparticles in pregnant rats and the effect on the biochemical profile in urine. J. Appl. Toxicol. http://dx.doi.org/10.1002/jat.3387.

Flint, O.P., 1983. A micromass culture method for rat embryonic neural cells. J. Cell Sci. 61, 247–262.

Grandjean, P., Landrigan, P.J., 2006. Developmental neurotoxicity of industrial chemicals. Lancet 368, 2167–2178. http://dx.doi.org/10.1016/S0140-6736(06)69665-7.

Hernandez, R.B., Farina, M., Esposito, B.P., et al., 2011. Mechanisms of manganese-induced neurotoxicity in primary neuronal cultures: the role of manganese speciation and cell type. Toxicol. Sci. 124, 414–423. http://dx.doi.org/10.1093/toxsci/kfr234.

Lammer, E.J., Chen, D.T., Hoar, R.M., et al., 1985. Retinoic acid embryopathy. N. Engl. J. Med. 313, 837–841. http://dx.doi.org/10.1056/NEJM198510033131401.

Leo, B.F., Chen, S., Kyo, Y., et al., 2013. The stability of silver nanoparticles in a model of pulmonary surfactant. Environ. Sci. Technol. 47, 11232–11240. http://dx.doi.org/10.1021/es403377p.

Levard, C., Hotze, E.M., Lowry, G.V., et al., 2012. Environmental transformations of silver nanoparticles: impact on stability and toxicity. Environ. Sci. Technol. 46, 6900–6914. http://dx.doi.org/10.1021/es2037405.

Loeschner, K., Hadrup, N., Qvortrup, K., et al., 2011. Distribution of silver in rats following 28 days of repeated oral exposure to silver nanoparticles or silver acetate. Part Fibre Toxicol. 8, 18. http://dx.doi.org/10.1186/1743-8977-8-18.

Ma, R., Levard, C., Marinakos, S.M., et al., 2012. Size-controlled dissolution of organic-coated silver nanoparticles. Environ. Sci. Technol. 46, 752–759. http://dx.doi.org/10.1021/es201686j.

Maden, M., 2007. Retinoic acid in the development, regeneration and maintenance of the nervous system. Nat. Rev. Neurosci. 8, 755–765. http://dx.doi.org/10.1038/nrn2212.

Maxwell, S.L., Li, M., 2005. Midbrain dopaminergic development in vivo and in vitro from embryonic stem cells. J. Anat. 207, 209–218. http://dx.doi.org/10.1111/j.1469-7580.2005.00453.x.

Miodovnik, A., 2011. Environmental neurotoxicants and developing brain. Mt Sinai J. Med. 78, 58–77. http://dx.doi.org/10.1002/msj.20237.

Morishita, Y., Yoshioka, Y., Takimura, Y., et al., 2016. Distribution of silver nanoparticles to breast milk and their biological effects on breast-fed offspring mice. ACS Nano 10, 8180–8191. http://dx.doi.org/10.1021/acsnano.6b01782.

Munusamy, P., Wang, C., Engelhard, M.H., et al., 2015. Comparison of 20 nm silver nanoparticles synthesized with and without a gold core: structure, dissolution in cell culture media, and biological impact on macrophages. Biointerphases 10, 031003. http://dx.doi.org/10.1116/1.4926547.

National Research Council Committee on Developmental Toxicology (2000). In (Eds.), Scientific Frontiers in Developmental Toxicology and Risk Assessment. Washington (DC): National Academies Press (US), Copyright 2000 by the National Academy of Sciences. All rights reserved. doi:http://dx.doi.org/10.17226/9871.

Oberdorster, G., Oberdorster, E., Oberdorster, J., 2005. Nanotoxicology: an emerging discipline evolving from studies of ultrafine particles. Environ. Health Perspect. 113, 823–839.

Park, J.J., Weldon, B.A., Hong, S., et al., 2017. Characterization of two 3d embryonic mouse midbrain micromass *in vitro* culture systems. Toxicol. in Vitro 48, 33–44.

Patchin, E.S., Anderson, D.S., Silva, R.M., et al., 2016. Size-dependent deposition, translocation, and microglial activation of inhaled silver nanoparticles in the rodent nose and brain. Environ. Health Perspect. http://dx.doi.org/10.1289/EHP234. (EHP234 [pii]).

Quadros, M.E., Pierson, R.T., Tulve, N.S., et al., 2013. Release of silver from nanotechnology-based consumer products for children. Environ. Sci. Technol. 47, 8894–8901. http://dx.doi.org/10.1021/es4015844.

Reidy, B., Haase, A., Luch, A., Dawson, K.A., Lynch, I., 2013. Mechanisms of Silver Nanoparticle Release, Transformation and Toxicity: A Critical Review of Current Knowledge and Recommendations for Future Studies and Applications. Materials 6 (6), 2295–2350 http://doi.org/10.3390/ma6062295.

Rice, D., Barone Jr., S., 2000. Critical periods of vulnerability for the developing nervous system: evidence from humans and animal models. Environ. Health Perspect. 108 (Suppl. 3), 511–533 (doi:sc271_5_1835 [pii]).

Robison, G., Sullivan, B., Cannon, J.R., et al., 2015. Identification of dopaminergic neurons of the substantia nigra pars compacta as a target of manganese accumulation. Metallomics 7, 748–755. http://dx.doi.org/10.1039/c5mt00023h.

Rodier, P.M., 1994. Vulnerable periods and processes during central nervous system development. Environ. Health Perspect. 102 (Suppl. 2), 121–124.

Rodier, P.M., 1995. Developing brain as a target of toxicity. Environ. Health Perspect. 103, 73–76. http://dx.doi.org/10.2307/3432351.

Scoville, D.K., Botta, D., Galdanes, K., et al., 2017. Genetic determinants of susceptibility to silver nanoparticle-induced acute lung inflammation in mice. FASEB J. 31, 4600–4611. http://dx.doi.org/10.1096/fj.201700187R.

Shannahan, J.H., Lai, X., Ke, P.C., et al., 2013. Silver nanoparticle protein corona composition in cell culture media. PLoS One 8, e74001. http://dx.doi.org/10.1371/journal.pone.0074001.

Sidhu, J.S., Ponce, R.A., Vredevoogd, M.A., et al., 2006. Cell cycle inhibition by sodium arsenite in primary embryonic rat midbrain neuroepithelial cells. Toxicol. Sci. 89, 475–484. http://dx.doi.org/10.1093/toxsci/kfj032.

Silbergeld, E.K., 1992. Mechanisms of lead neurotoxicity, or looking beyond the lamppost. FASEB J. 6, 3201–3206.

Stebounova, L.V., Adamcakova-Dodd, A., Kim, J.S., et al., 2011. Nanosilver induces minimal lung toxicity or inflammation in a subacute murine inhalation model. Part. Fibre Toxicol. 8, 5. http://dx.doi.org/10.1186/1743-8977-8-5.

Stern, S.T., Adiseshaiah, P.P., Crist, R.M., 2012. Autophagy and lysosomal dysfunction as emerging mechanisms of nanomaterial toxicity. Particle Fibre Toxicol. 9, 20. http://dx.doi.org/10.1186/1743-8977-9-20.

Tang, J., Xiong, L., Wang, S., et al., 2009. Distribution, translocation and accumulation of silver nanoparticles in rats. J. Nanosci. Nanotechnol. 9, 4924–4932.

Tang, J., Xiong, L., Zhou, G., et al., 2010. Silver nanoparticles crossing through and distribution in the blood-brain barrier in vitro. J. Nanosci. Nanotechnol. 10, 6313–6317.

The R Core Team, 2013. R: A Language and Environment for Statistical Computing. R Foundation for Statistical Computing, Vienna, Austria.

Thomas, D.G., Smith, J.N., Thrall, B.D., et al., 2018. Isd3: a particokinetic model for predicting the combined effects of particle sedimentation, diffusion and dissolution on cellular dosimetry for in vitro systems. Part. Fibre Toxicol. 15, 6. http://dx.doi.org/10.1186/s12989-018-0243-7.

Tulve, N.S., Stefaniak, A.B., Vance, M.E., et al., 2015. Characterization of silver nanoparticles in selected consumer products and its relevance for predicting children's potential exposures. Int. J. Hyg. Environ. Health 218, 345–357. http://dx.doi.org/10.1016/j.ijheh.2015.02.002.

Utembe, W., Potgieter, K., Stefaniak, A.B., et al., 2015. Dissolution and biodurability: important parameters needed for risk assessment of nanomaterials. Part. Fibre Toxicol. 12, 11. http://dx.doi.org/10.1186/s12989-015-0088-2.

Wang, X., Ji, Z., Chang, C.H., et al., 2014. Use of coated silver nanoparticles to understand the relationship of particle dissolution and bioavailability to cell and lung toxicological potential. Small 10, 385–398. http://dx.doi.org/10.1002/smll.201301597.

Whittaker, S.G., Faustman, E.M., 1991. Effects of albendazole and albendazole sulfoxide on cultures of differentiating rodent embryonic cells. Toxicol. Appl. Pharmacol. 109, 73–84.

Whittaker, S.G., Wroble, J.T., Silbernagel, S.M., et al., 1993. Characterization of cytoskeletal and neuronal markers in micromass cultures of rat embryonic midbrain cells. Cell Biol. Toxicol. 9, 359–375.

Wildt, B.E., Celedon, A., Maurer, E.I., et al., 2016. Intracellular accumulation and dissolution of silver nanoparticles in l-929 fibroblast cells using live cell time-lapse microscopy. Nanotoxicology 10, 710–719. http://dx.doi.org/10.3109/17435390.2015.1113321.

Yang, Z., Liu, Z.W., Allaker, R.P., et al., 2010. A review of nanoparticle functionality and toxicity on the central nervous system. J. R. Soc. Interface 7 (Suppl. 4), S411–422. http://dx.doi.org/10.1098/rsif.2010.0158.focus.